Geometry sensing by self-organized protein patterns

Supporting Information

Jakob Schweizer[1‡], Martin Loose[1,4‡], Mike Bonny[2], Karsten Kruse[2], Ingolf Mönch,[3] and Petra Schwille[1*]

June 29, 2012

[1]Biophysics, BIOTEC, Dresden University of Technology, Tatzberg 47-51, 01307 Dresden, Germany

[2]Theoretische Physik, Universität des Saarlandes, Saarbrücken, Germany

[3]Institute for Integrative Nanosciences, IFW Dresden, Helmholtz Strasse 20, 01069 Dresden, Germany

[4]Department for Systems Biology, Harvard Medical School, 200 Longwood Avenue, Boston, MA 02115, USA

[‡]These authors contributed equally.

[*]To whom correspondence should be addressed: E-mail: petra.schwille@biotec.tu-dresden.de (P.S.) and martin_loose@hms.harvard.edu (M.L.)

Supplementary Text

Dynamic equations

We describe the dynamics of the Min proteins on structured membranes by using a deterministic mean-field description. In this model, we assume that binding of MinD to the membrane is cooperative, that MinE binds to membrane-bound MinD, and that MinE induces detachment of MinD from the membrane [1–3]. It extends previous models in that it accounts for transient binding of MinE to the membrane after MinE-induced MinD detachment [4, 5]. To alleviate the numerical calculations, we neglect the dimension perpendicular to the flat membrane in our description. We have checked on specific examples that the same phenomena as reported below can also be observed in the full three-dimensional description.
The distributions of MinD and MinE in the buffer are given by the densities c_D and c_E. The distributions of MinD, MinDE-complexes, and MinE on the membrane are, respectively, denoted by c_d, c_{de}, and c_e. The dynamic equations read

$$\partial_t c_D = D_D \Delta c_D - c_d(\omega_D + \omega_{dD} c_d)(c_{\max} - c_d - c_{de})/c_{\max} + (\omega_{de,m} + \omega_{de,c}) c_{de} \tag{1}$$

$$\partial_t c_E = D_E \Delta c_E - \omega_E c_E c_d + \omega_{de,c} c_{de} + \omega_e c_e \tag{2}$$

$$\partial_t c_d = D_d \Delta c_d + c_d(\omega_D + \omega_{dD} c_d)(c_{\max} - c_d - c_{de})/c_{\max} - \omega_E c_E c_d - \omega_{ed} c_e c_d \tag{3}$$

$$\partial_t c_{de} = D_{de} \Delta c_{de} + \omega_E c_E c_d + \omega_{ed} c_e c_d - (\omega_{de,m} + \omega_{de,c}) c_{de} \tag{4}$$

$$\partial_t c_e = D_e \Delta c_e + \omega_{de,m} c_{de} - \omega_{ed} c_e c_d - \omega_e c_e \quad . \tag{5}$$

Here, Δ denotes the Laplace operator in two dimensions. For the meaning of the parameters and their values refer to Table S1.
The equations for c_d, c_{de}, and c_e are solved on 2d domains that correspond to the structure of the membrane patches in the corresponding experiment. Accordingly, the terms describing protein attachment to and detachment from the membrane in Eqs. (1)-(5) are restricted to these regions, too. For the diffusion terms in Eqs. (3)-(5) we use no flux conditions at the boundaries of the membrane domains. Finally, periodic boundary conditions are imposed on c_D and c_E.

D_D	$50\frac{\mu\mathrm{m}^2}{s}$	Diffusion constant of unbound MinD
D_E	$50\frac{\mu\mathrm{m}^2}{s}$	Diffusion constant of unbound MinE
D_d	$0.24\frac{\mu\mathrm{m}^2}{s}$	Diffusion constant of membrane-bound MinD
D_{de}	$0.24\frac{\mu\mathrm{m}^2}{s}$	Diffusion constant of membrane-bound MinDE complexes
D_e	$0.48\frac{\mu\mathrm{m}^2}{s}$	Diffusion constant of membrane-bound MinE
ω_D	$0.045\frac{1}{s}$	Rate of spontaneous attachment of cytosolic MinD
ω_{dD}	$9\,10^{-4}\frac{\mu\mathrm{m}^2}{s}$	Measure for the degree of cooperativity in the attachment of cytosolic MinD
ω_E	$5\,10^{-4}\frac{\mu\mathrm{m}^2}{s}$	Rate of cytosolic MinE binding to membrane-bound MinD
ω_{ed}	$2.5\,10^{-3}\frac{\mu\mathrm{m}^2}{s}$	Rate of association of membrane-bound MinD and membrane-bound MinE
$\omega_{de,m}$	$0.8\frac{1}{s}$	Rate of MinD detachment with MinE staying on the membrane
$\omega_{de,c}$	$0.08\frac{1}{s}$	Rate of MinD detachment with MinE leaving the membrane
ω_e	$0.08\frac{1}{s}$	Rate of MinE detachment
$c_{\max}$	$2\,10^4\frac{1}{\mu\mathrm{m}^2}$	Maximal concentration of membrane-bound MinD
C_{D0}	$2.9\,10^3\frac{1}{\mu m^2}$	Total MinD concentration
C_{E0}	$1.9\,10^3\frac{1}{\mu m^2}$	Total MinE concentration

Table S1: Meaning of the parameters present in Eqs. (1)-(5) and their values used in the simulations.

We solve the dynamic equations (1)-(5) by using Comsol Multiphysics 4.1® which is a solver for partial differential equations based on the finite element method (FEM). For all calculations, we use the parameter values given in Table S1.

Origin of fluctuations in Fig. 5

Since our model is deterministic, it might come as a surprise that the graphs in Fig. 5A-C of the main text are noisy. There are two reasons for these fluctuations. On one hand for the numerical solution of the dynamic equations we need to discretize space. On the other hand, the spiral defect sending out the wave fronts moves slowly. As a consequence the wave fronts all differ somewhat. To reduce the fluctuations, we have averaged over several points in time. Error bars give the standard deviation for the corresponding distributions.

Supplementary Figures

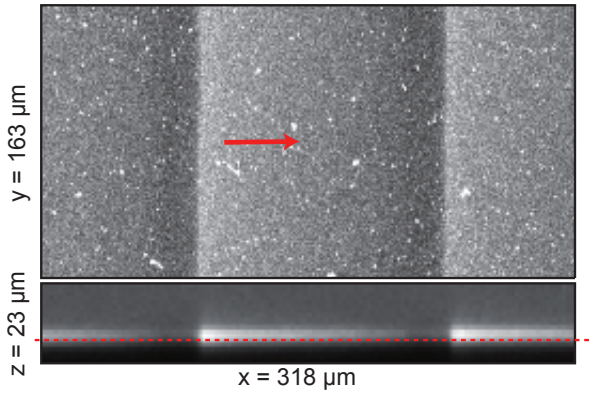

Figure S1 : Min proteins are confined to a narrow region above the membrane. Top: micrograph of traveling wave patterns. Bottom: corresponding z-stack of waves. The red line corresponds to the z-position of the membrane.

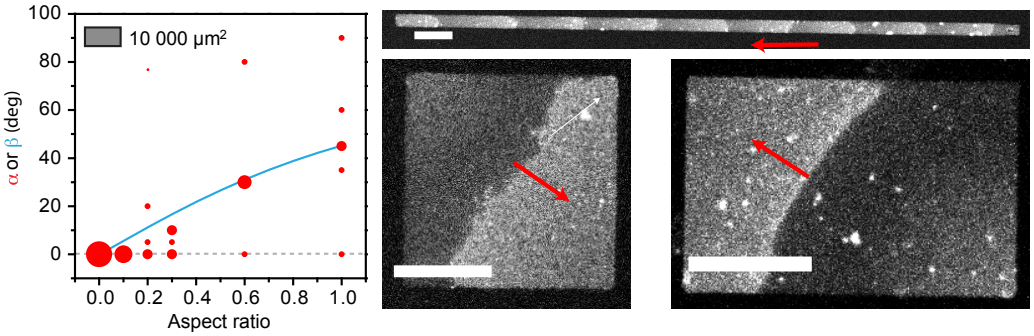

Figure S2 : Protein waves preferentially travel along the longest possible path. Protein waves also align along the diagonal of larger rectangular membrane patches. However, compared to small rectangular membranes (Fig. 2 in main text), alignment is less precise. Scale bars are 50 μm.

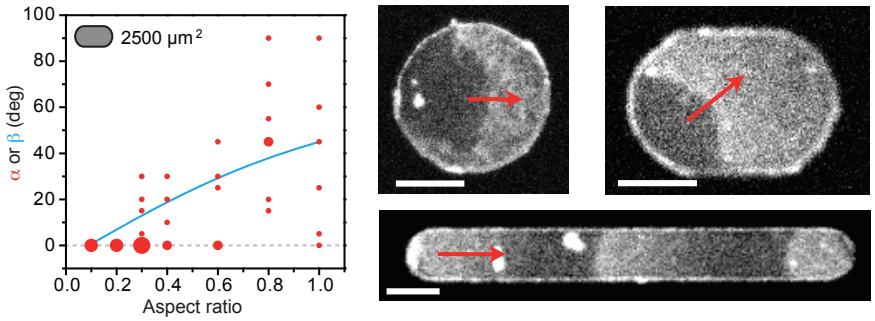

Figure S3 : Protein waves always align along the longest possible path. On membrane patches with round ends, the longest path the waves can travel is always parallel to the long axis. As a result, protein waves travel with an angle of 0 degrees also at aspect ratios higher than 0.3. If the membrane patches are completely round any preferred orientation is lost. Scale bars are 50 μm.

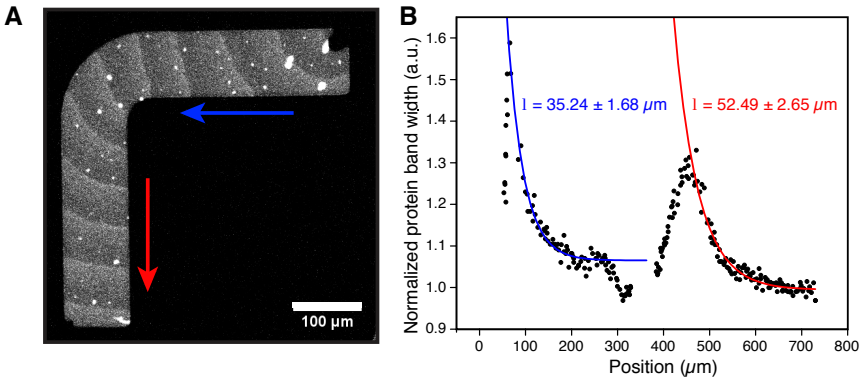

Figure S4 : Steering of protein waves on L-shaped membrane patches. **(A)** Micrograph of protein waves traveling along an L-shaped membrane **(B)** Normalized width of the protein bands shown in **A**. The characteristic length scale of alignment is shorter than the wavelength. Blue and red curves represent alignment in the first and second leg of the L-shaped membrane, respectively.

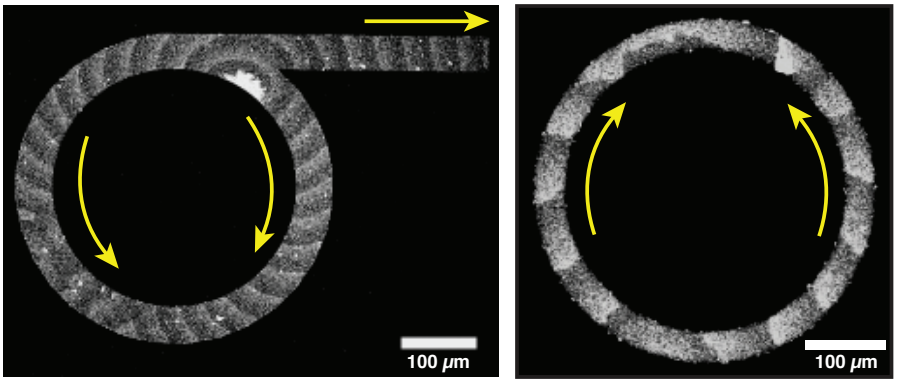

Figure S5 : Steering of protein waves on circular membrane patches. Protein waves readily adapt to changes of the flat membrane geometry: on straight segments they follow the linear pathway whereas in circular structures waves propagate along the curved pathway. On a simple ring, two waves that emerge from the same source meet at the opposite side where they annihilate each other.

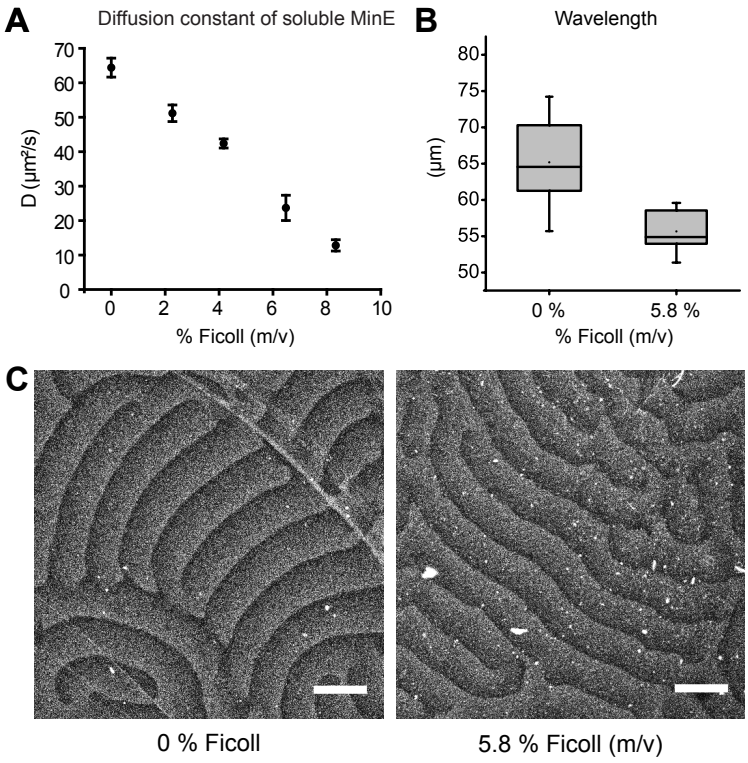

Figure S6 : Effect of molecular crowding on protein waves. (A) Molecular crowding after addition of Ficoll reduces the diffusion of Min proteins in bulk as measured by FCS. (B) In the presence of 6 % (m/v) Ficoll, the wavelength decreased about 14 % (from about 65 μm to about 56 μm). (C) Corresponding micrographs of traveling waves in the absence and presence of Ficoll. Scale bars are 50 μm.

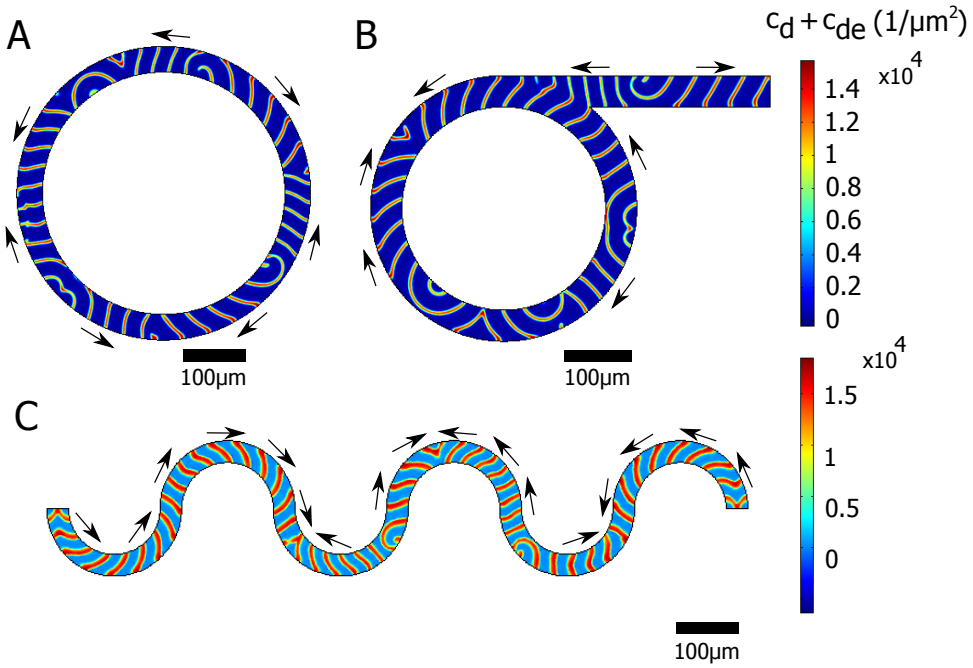

Figure S7 : Simulations of Min protein waves on different membrane geometries. As in our experiments, protein waves follow the path of the membrane: (A) circles, (B) synchrotron-like geometries and (C) serpentine structures.

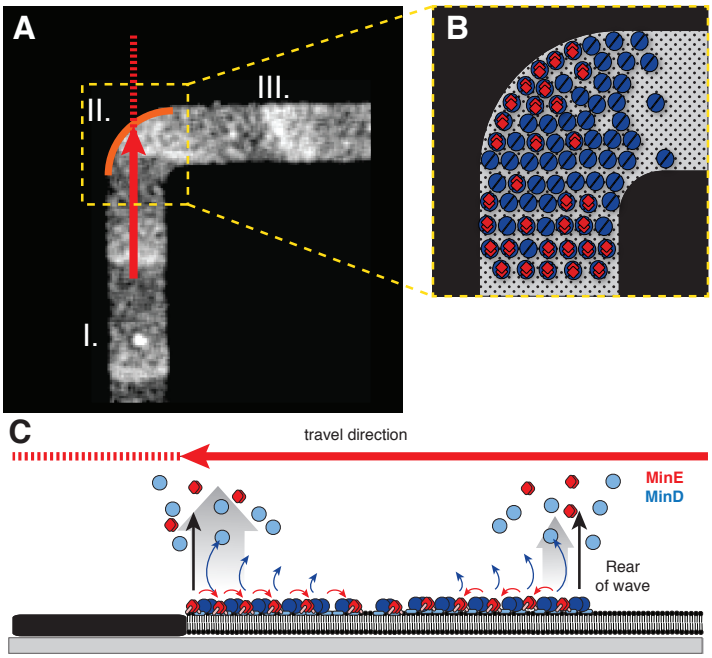

Figure S8 : Change of direction of Min protein waves. A) Micrograph corresponding to Fig. 3A of the main text. B) Schematic illustration of the protein wave at the position of the bend. C) Corresponding cross section. Following its initial path (red arrow and dashed line), the protein waves run into the gold boundary at the knee of the membrane. Here, MinD (blue) is induced to leave the membrane, while MinE (red) can remain bound to the membrane. Due to spatial confinement, diffusion of membrane-bound MinE is restricted and can only diffuse towards the rear of the wave, where the MinE/MinD ratio is already high. As a consequence, MinD is removed at a higher rate, thus further increasing the MinE/MinD ratio and accelerating MinD detachment and wave propagation close to the boundary. This effect always occurs if the wave is following a path towards the membrane (and therefore not at the inner side of the bend), leading to effective alignment of the protein wave.

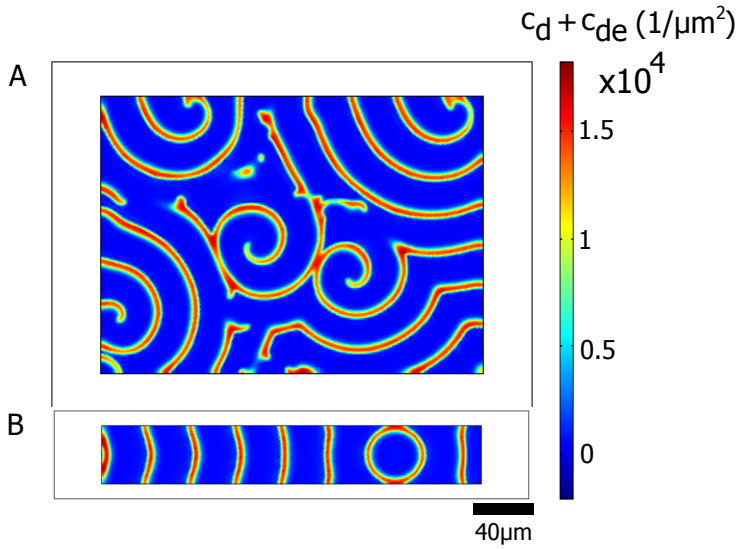

Figure S9 : Influence of confinement on Min-protein waves in our theoretical model. (A) For membrane patches with an extension of several wavelengths in both directions, the confinement has no visible influence of pattern formation. (B) For patches with a width that is smaller or of the same size as the wavelength, the waves are guided by the lateral confinement. Figure corresponds to Fig. 1B of the main text.

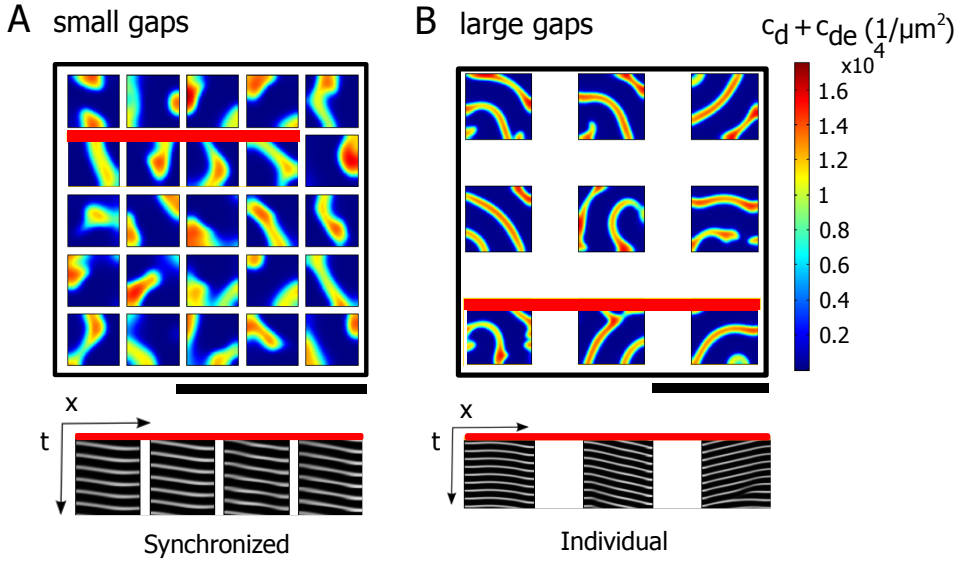

Figure S10 : Coupling of waves across barriers with different distances. Figure corresponds to Fig. 4A of the main text. Scale bars are 100μm.

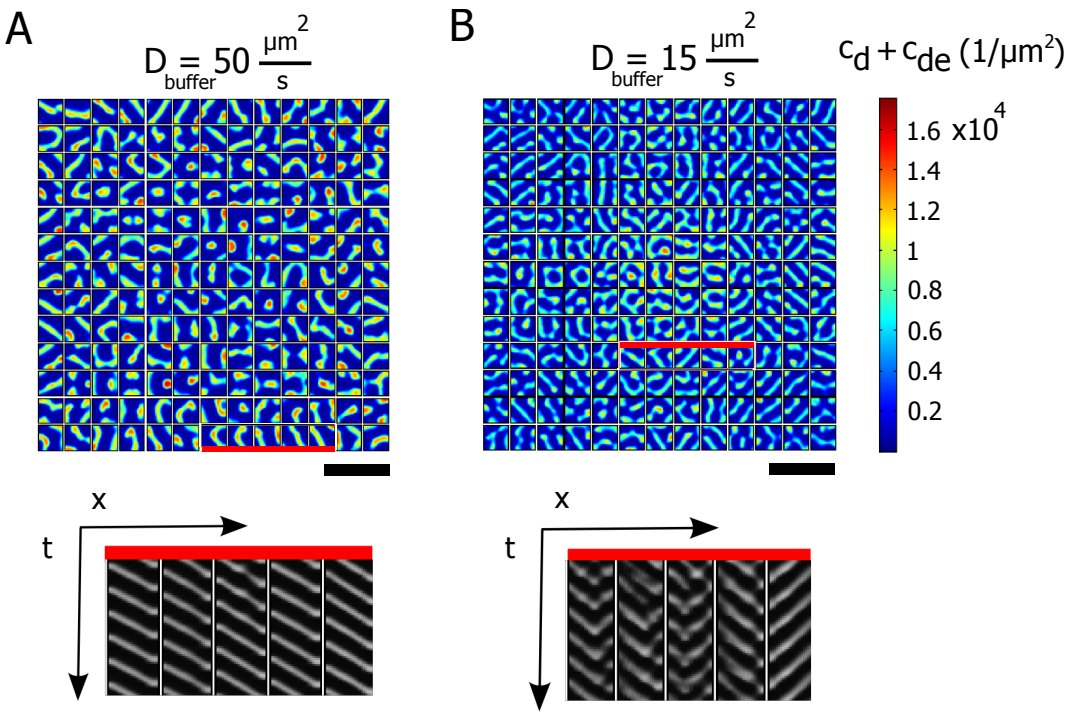

Figure S11 : Coupling of waves across barriers for different diffusion constants. For sufficiently small diffusion constants ($D \leq 20\mu m^2/s$) (B), patterns in different patches are not coupled between neighboring patches. Kymographs show the time evolution of the MinD concentration profile along red lines. Scale bars are 100 μm. Figure corresponds to Fig. 4B of the main text. Scale bars are 100μm.

Supplementary Movie Captions

Supplementary Movie 1: Confocal fluorescence micrographs of Cy5-labeled MinE in Min protein waves on membrane checkerboard patterns (MinD = 0.8 μM, MinE = 0.5 μM with 10 mol % MinE-Cy5). Scale bar is 100 μm.

Supplementary Movie 2: Confocal fluorescence micrographs of Cy5-labeled MinE in Min protein waves on rectangular membranes with different aspect ratios (MinD = 0.8 μM, MinE = 0.5 μM with 10 mol % MinE-Cy5). Scale bar is 100 μm.

Supplementary Movie 3: Confocal fluorescence micrographs of Cy5-labeled MinE in Min protein waves on membranes with different shapes (MinD = 0.8 μM, MinE = 0.5 μM with 10 mol % MinE-Cy5). Scale bar is 100 μm.

Supplementary Movie 4: Confocal fluorescence micrographs of Cy5-labeled MinE in Min protein waves on membrane patches separated by constant distances and in the presence and absence of 6% (m/v) Ficoll (MinD = 0.8 μM, MinE = 0.5 μM with 10 mol % MinE-Cy5). Scale bar is 100 μm.

Supplementary Movie 5: Theoretical reproduction of Min protein waves on a L-shaped membrane. Time shown is in seconds.

Supplementary Movie 6: Theoretical reproduction of Min protein waves on various membrane geometries.

Supplementary Movie 7: Theoretical reproduction of Min protein waves on membrane patches with different aspect ratios.

Supplementary Movie 8: Theoretical reproduction of diffusive coupling at different diffusion constants of the proteins in solution.

Supplementary Movie 9: Simulation of cytoplasmic protein densities using our theoretical model.

Bibliography

1. H. Meinhardt and P. A. de Boer. Pattern formation in Escherichia coli: a model for the pole-to-pole oscillations of Min proteins and the localization of the division site. Proc Natl Acad Sci USA, 98: 14202-7, 2001.

2. K. C. Huang, Y. Meir, and N. S. Wingreen. Dynamic structures in Escherichia coli: spontaneous formation of MinE rings and MinD polar zones. Proc Natl Acad Sci USA, 100: 12724-8, 2003.

3. M. Loose, E. Fischer-Friedrich, J. Ries, K. Kruse, and P. Schwille. Spatial regulators for bacterial cell division self-organize into surface waves in vitro. Science, 320: 789-92, 2008.

4. M. Loose, E. Fischer-Friedrich, C. Herold, K. Kruse, and P. Schwille. Min protein patterns emerge from rapid rebinding and membrane interaction of MinE. Nat Struct & Mol Biol, 577-83, 2011.

5. K. Park, W. Wu, K. P. Battaile, S. Lovell, T. Holyoak, and J. Lutkenhaus. The Min oscillator uses MinD-dependent conformational changes in MinE to spatially regulate cytokinesis. Cell, 146: 396-407, 2011.